Junior researchers

ახალგაზრდა მკვლევარები

Vol. 4 Issue 2, 2026

https://doi.org/10.52340/jr.2026.04.02.20



# Synthesis, Spectroscopic Characterization and Molecular Docking of Dibenzylideneacetone and Its 4,4′-Dichloro and 4,4′-Dinitro Analogues as Potential Aldose Reductase Ligands

**Mariam Urushadze[1], Nino Nikoleishvili[2], Elene Katsadze[3]**

Iv. Javakhishvili Tbilisi state university, Tbilisi, Georgia

[1]BSc in Chemistry, department of chemistry of Organic and Natural compounds, mariam.urushadze688@ens.tsu.edu.ge; [2]Assistant-professor, department of chemistry of Organic and Natural compounds, nino.nikoleishvili@tsu.ge; [3]Associate professor, department of chemistry of Organic and Natural compounds, elene.katsadze@tsu.ge , https://orcid.org/0009-0003-0327-2917

**Abstract:**

Dibenzylideneacetone (DBA) and its analogues are cross-conjugated bis-chalcones with a broad range of biological and photophysical properties. Here, DBA (**3a**) and its 4,4′-dichloro (**3b**) and 4,4′-dinitro (**3c**) analogues were prepared by base-catalysed Claisen–Schmidt condensation of acetone (**1**) with the corresponding *para*-substituted benzaldehydes (**2a–c**) in aqueous ethanolic sodium hydroxide. After recrystallization, the compounds were isolated in yields of 65% (**3a**), 57% (**3b**) and 52% (**3c**). FT-IR and $^1$H NMR data, in particular the olefinic coupling constants of 15.9–16.0 Hz, are consistent with the (1*E*,4*E*) configuration of all three products. In chloroform (10 μg/mL), the UV–Vis absorption maxima ($\lambda_{max}$) were observed at 330.6 nm (**3a**), 338 nm (**3b**) and 335 nm (**3c**). The compounds were docked into the active site of porcine aldose reductase (PDB ID: 1AH0) with AutoDock 4.2.6, which gave binding free energies of –7.42, –7.43 and –6.89 kcal/mol (estimated $K_i$ of 3.62, 3.58 and 8.92 μM) for **3a**, **3b** and **3c**, respectively. The top-ranked poses differ in their non-covalent contacts: **3a** forms a hydrogen bond with His163 together with π–π T-shaped, π–cation and π–alkyl interactions; **3b** forms a hydrogen bond with His163, a Cl···O/N halogen contact with Asn292, and π–σ and π–alkyl interactions; and **3c** forms hydrogen bonds with Thr A:191 and His163 and a π–anion contact with Glu193. Because the differences in docking score (0.01–0.54 kcal/mol) are smaller than the usual uncertainty of empirical scoring functions (about 1–2 kcal/mol), the three compounds should be regarded as having comparable predicted affinity. The docking models provide a starting point for molecular dynamics simulations and *in vitro* aldose reductase inhibition assays.

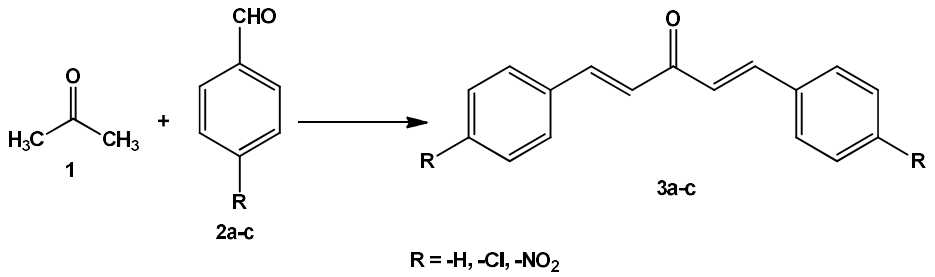
***Keywords:*** dibenzylideneacetone; Claisen–Schmidt condensation; bis-chalcone; molecular docking; aldose reductase

## 1. Introduction

Dibenzylideneacetone (DBA) and its substituted analogues are symmetrical bis-chalcones. Like other members of the chalcone family, they are built around a cross-conjugated α,β-unsaturated carbonyl system [1,2]. This dienone unit is electrophilic and acts as a soft Michael acceptor towards biological nucleophiles, which is generally held responsible for much of the pharmacological activity of these compounds. Chalcone-type compounds have been reported to show anti-inflammatory, antioxidant and radical-scavenging effects, which are often invoked to explain their neuroprotective properties [2,4], as well as antiproliferative activity and antimicrobial activity directed mainly at Gram-positive bacteria and pathogenic fungi [1,2]. Outside medicinal chemistry, the extended π-conjugation of DBA derivatives gives strong absorption in the ultraviolet region, which has attracted interest in UV-filter and polymer-stabilizer applications [3]. Symmetrical bis-α,β-unsaturated ketones are also ersatile precursors. The central carbonyl group can, in principle, be condensed with primary amines to give azomethines (Schiff bases, –C=N–), a motif found in many antibacterial, antiviral and antitumour agents [5–7]. We therefore regard functionalized DBA derivatives as potential precursors of π-conjugated, polyfunctional Schiff bases. As a first step in this direction, we prepared three representative symmetrical analogues (**3a–c**) by Claisen–Schmidt condensation, the most direct and atom-economical route to α,β-unsaturated ketones [6,7].

Besides serving as synthetic precursors, the DBA scaffold may also be of biological interest. Aldose reductase (AR) is an NADPH-dependent aldo-keto reductase that catalyses the first step of the polyol pathway, the reduction of glucose to sorbitol. Under hyperglycaemic conditions its activity has been implicated in the chronic complications of diabetes and, more recently, in oxidative and inflammatory signalling, and the enzyme has long been a target for inhibitor design [8]. Chalcone-type compounds have also been studied under high-glucose conditions [4]. DBA (**3a**) and its 4,4′-dichloro (**3b**) and 4,4′-dinitro (**3c**) analogues are known compounds, but, to our knowledge, their interaction with AR has not been examined. Here, we describe the preparation of **3a–c** by base-catalysed Claisen–Schmidt condensation of acetone (**1**) with benzaldehyde, 4-chlorobenzaldehyde and 4-nitrobenzaldehyde (**2a–c**) (**Scheme 1**), their characterization by FT-IR, NMR and UV–Vis spectroscopy, and a comparative docking study against AR to examine how the *para* substituent affects the predicted binding mode. Although the reaction is simple in principle, isolated yields can depend on temperature and substrate solubility, particularly with strongly electron-withdrawing groups.

**Scheme 1.** Synthesis of symmetrical dibenzylideneacetones **3a–c** (R = H, 4-Cl, 4-$NO_2$) by base-catalysed Claisen–Schmidt condensation of acetone (**1**) with benzaldehydes **2a–c**.



## 2. Experimental

### 2.1. General methods

All reagents and solvents were purchased from Sigma-Aldrich and used as received. Melting points were measured in open capillaries on a BMP-1 apparatus (BioBase) and are uncorrected. $^{1}$H NMR (400 MHz) and $^{13}$C NMR (101 MHz) spectra were recorded in $CDCl_3$ on a Bruker Avance 400 spectrometer; chemical shifts ($\delta$) are given in ppm relative to the residual solvent signal and coupling constants ($J$) in Hz. FT-IR spectra were recorded on an Cary 630 FTIR spectrometer using KBr pellets. UV–Vis absorption spectra were measured in $CHCl_3$ (10 μg/mL) on an Agilent Cary 60 spectrophotometer. Reactions were monitored by thin-layer chromatography (TLC) on pre-coated silica gel 60 $F_{254}$ plates (Merck), with detection under UV light (254 nm).

### 2.2. General procedure for the synthesis of dibenzylideneacetones (3a–c)

A 10% (w/v) aqueous solution of sodium hydroxide (250 mmol) and ethanol (100 mL) were placed in a 250 mL Erlenmeyer flask, cooled to 20–30 °C in a water bath and stirred vigorously with a magnetic stirrer. A solution of the appropriate benzaldehyde **2a–c** (100 mmol) and acetone (**1**, 50 mmol) was prepared separately, and about half of it was added dropwise to the alkaline medium. A yellow precipitate of the crude product appeared within a few minutes. After 15 min of stirring, the remaining aldehyde–acetone mixture was added and stirring was continued vigorously for a further 30 min at ambient temperature (20–30 °C). For 4-nitrobenzaldehyde (**2c**), the mixture was kept at 35 °C so that the aldehyde dissolved completely. The solid was collected by vacuum filtration on a Büchner funnel, washed with ice-cold distilled water until the washings were neutral, and dried to constant weight. Recrystallization from ethyl acetate gave pure **3a–c**.

### 2.3. Spectroscopic and physical data for compounds (3a–c)

**(1*E*,4*E*)-1,5-Diphenylpenta-1,4-dien-3-one (3a).** Yellow crystalline solid; yield 65%; m.p. 110–112 °C; IR (KBr, cm$^{-1}$): 3025 (Ar C–H), 1648 (C=O), 1597 (C=C), 1494, 1446 (Ar C=C), 1331, 1100, 1071, 979 (*trans* CH=CH), 922, 802, 750, 690 (monosubstituted phenyl); UV–Vis ($CHCl_3$): $\lambda_{max}$ = 330.6 nm; $^{1}$H NMR (400 MHz, $CDCl_3$): $\delta$ 7.77 (d, $J$ = 15.9 Hz, 2H), 7.69–7.60 (m, 4H), 7.49–7.39 (m, 6H), 7.12 (d, $J$ = 16.0 Hz, 2H); $^{13}$C NMR (101 MHz, $CDCl_3$): $\delta$ 188.97, 143.84, 134.84, 130.55, 129.01, 128.44, 125.47.

**(1*E*,4*E*)-1,5-Bis(4-chlorophenyl)penta-1,4-dien-3-one (3b).** Yellow crystalline solid; yield 57%; m.p. 190–191 °C; IR (KBr, cm$^{-1}$): 1652 (C=O), 1603, 1584 (C=C), 1189, 1068, 1008, 980 (*trans* CH=CH), 815 (1,4-disubstituted ring, C–H out-of-plane bending), 730; UV–Vis ($CHCl_3$): $\lambda_{max}$ = 338 nm; $^{1}$H NMR (400 MHz, $CDCl_3$): $\delta$ 7.70 (d, $J$ = 16.0 Hz, 2H), 7.60–7.52 (m, 4H), 7.45–7.35 (m, 4H), 7.05 (d, $J$ = 15.9 Hz, 2H); $^{13}$C NMR (101 MHz, $CDCl_3$): $\delta$ 188.37, 142.08, 136.54, 133.23, 129.58, 129.31, 125.73.

**(1*E*,4*E*)-1,5-Bis(4-nitrophenyl)penta-1,4-dien-3-one (3c).** Yellow-orange crystalline solid; yield 52%; m.p. 246–247 °C; IR (KBr, cm$^{-1}$): 1648 (C=O), 1602 (C=C), 1524 ($NO_2$ asym.), 1343 ($NO_2$), 1109, 999 (*trans* CH=CH), 851 (1,4-disubstituted ring); UV–Vis ($CHCl_3$): $\lambda_{max}$ = 335 nm; $^{1}$H NMR (400 MHz, $CDCl_3$): $\delta$ 8.32 (d, $J$ = 8.8 Hz, 4H), 7.85–7.77 (m, 6H), 7.20 (d, $J$ = 16.0 Hz, 2H); $^{13}$C NMR (101 MHz,

$CDCl_3$): $\delta$ 187.47, 148.79, 141.53, 140.62, 140.31, 138.72, 130.52, 130.32, 129.82, 129.04, 128.96, 128.47, 126.53, 124.33, 124.29.

### 2.4. Molecular docking

#### 2.4.1. Protein and ligand preparation

The X-ray structure of porcine aldose reductase in complex with $NADP^+$ and sorbinil (PDB ID: 1AH0; resolution 2.30 Å) [8-9] was downloaded from the RCSB Protein Data Bank. In Discovery Studio Visualizer 2021, the crystallographic water molecules and the co-crystallized inhibitor were removed and the $NADP^+$ cofactor was retained. Polar hydrogen atoms and Kollman united-atom charges were added, and the receptor was briefly energy-minimized to relieve steric clashes. The grid box was centred on the binding site of the co-crystallized ligand ($x$ = 18.129, $y$ = –1.872, $z$ = 17.450 Å) and had dimensions of 60 × 60 × 60 points with a spacing of 0.375 Å. The ligands **3a–c** were drawn in ChemDraw Professional 20.0, energy-minimized with the MM2 force field and saved in PDB format. Gasteiger partial charges were calculated and the rotatable bonds were defined before docking. Residue labels in the text, tables and figures refer to chain A of the prepared 1AH0 structure.

#### 2.4.2. Docking protocol

Docking was performed with AutoDock 4.2.6 using the Lamarckian genetic algorithm (LGA). For each ligand, 100 independent LGA runs were carried out with a population size of 150, a maximum of $2.5 \times 10^6$ energy evaluations, a maximum of 27,000 generations, a gene mutation rate of 0.02 and a crossover rate of 0.80. The resulting poses were clustered with an RMSD tolerance of 2.0 Å. Binding free energies ($\Delta G$) and theoretical inhibition constants ($K_i$) were evaluated at 298.15 K.

## 3. Results and Discussion

### 3.1. Synthesis

Compounds **3a–c** were prepared by base-catalysed Claisen–Schmidt condensation of acetone (**1**) with two equivalents of the corresponding aromatic aldehyde (**2a–c**) in aqueous ethanolic NaOH. Keeping the temperature between 20 and 30 °C was important for clean conversion. At lower temperatures the mono-condensation intermediate, benzalacetone, precipitated prematurely, whereas above 30 °C aldol self-condensation and resinification became competing processes. 4-Nitrobenzaldehyde (**2c**) was an exception: because of its low solubility in the reaction medium, the mixture was warmed to 35 °C to obtain a homogeneous solution. After TLC monitoring and recrystallization, **3a**, **3b** and **3c** were isolated in 65%, 57% and 52% yield, respectively.

### 3.2. Spectroscopic characterization

The FT-IR spectra of all three compounds are consistent with a cross-conjugated (1*E*,4*E*)-dienone. The C=O stretching bands of the conjugated ketone appear at 1648 $cm^{-1}$ (**3a**), 1652 $cm^{-1}$ (**3b**) and 1648

cm$^{-1}$ (**3c**), well below the value for saturated aliphatic ketones (about 1715 cm$^{-1}$), as expected for a carbonyl group conjugated with both styryl arms. The aromatic and olefinic =C–H stretching band of **3a** is found at 3025 cm$^{-1}$, and the out-of-plane C–H bending bands typical of *trans*-disubstituted alkenes occur at 979 (**3a**), 980 (**3b**) and 999 cm$^{-1}$ (**3c**). Substituent-related bands support the assignments: the out-of-plane C–H bending band of the 1,4-disubstituted ring at 815 cm$^{-1}$ for **3b**, and the asymmetric and symmetric $NO_2$ stretching bands at 1524 and 1343 cm$^{-1}$ for **3c**.

The $^1$H NMR spectra confirm the symmetrical (1*E*,4*E*) structure. In DBA (**3a**), the α- and β-olefinic protons give doublets at $\delta$ 7.12 ($J$ = 16.0 Hz) and 7.77 ($J$ = 15.9 Hz), respectively. Coupling constants of this size are typical of *trans* alkenes. The phenyl protons give multiplets between $\delta$ 7.39 and 7.69. The 4,4′-dichloro derivative **3b** shows analogous *trans*-olefinic doublets at $\delta$ 7.05 ($J$ = 15.9 Hz) and 7.70 ($J$ = 16.0 Hz), together with aromatic multiplets at $\delta$ 7.35–7.60. In the strongly electron-deficient 4,4′-dinitro compound **3c**, the aromatic protons *ortho* to the nitro groups are shifted downfield to $\delta$ 8.32 (d, $J$ = 8.8 Hz, 4H). The α-olefinic protons give a doublet at $\delta$ 7.20 ($J$ = 16.0 Hz, 2H), and the β-olefinic protons overlap with the remaining aromatic signals at $\delta$ 7.77–7.85. The $^{13}$C NMR spectra of **3a** and **3b** show the seven signals expected for a symmetrical molecule, with the carbonyl carbon at $\delta$ 188.97 and 188.37, respectively.

In chloroform, the longest-wavelength π→π* absorption maxima ($\lambda_{max}$) are at 330.6 nm for **3a**, 338 nm for **3b** and 335 nm for **3c**. Relative to the parent compound, the *para* substituents therefore cause only a small bathochromic shift of 4.4–7.4 nm. The larger shift is observed for the chloro rather than the nitro derivative, so no simple correlation with the electronic effect of the substituent can be drawn from these three compounds.

### 3.3. Molecular docking results

All three compounds docked favourably into the active-site cavity of porcine aldose reductase (PDB ID: 1AH0), with predicted binding free energies between –6.89 and –7.43 kcal/mol (**Table 1**). The top-ranked poses of DBA (**3a**; –7.42 kcal/mol, $K_i$ = 3.62 μM) and the 4,4′-dichloro derivative (**3b**; –7.43 kcal/mol, $K_i$ = 3.58 μM) have practically identical scores, whereas the 4,4′-dinitro analogue **3c** scores slightly lower (–6.89 kcal/mol, $K_i$ = 8.92 μM). The difference between **3a** and **3b** (0.01 kcal/mol) and the difference of about 0.5 kcal/mol for **3c** are both well within the roughly 1–2 kcal/mol error usually associated with the empirical scoring function of AutoDock, so the three compounds should be regarded as having comparable predicted affinity.

**Table 1.** AutoDock-predicted binding free energies (Δ*G*), estimated inhibition constants (*K*i) and cluster RMSD values for the top three conformational clusters of **3a–c** in porcine aldose reductase (PDB ID: 1AH0).

| Compound | Pose rank | ΔG (kcal/mol) | Estimated Ki (μM)[a] | RMSD from top-ranked pose (Å) |
|---|---|---|---|---|
| **3a** | 1 (top) | –7.42 | 3.62 | 0.00 |
| **3a** | 2 | –6.95 | — | 0.87 |
| **3a** | 3 | –6.51 | — | 1.12 |
| **3b** | 1 (top) | –7.43 | 3.58 | 0.00 |
| **3b** | 2 | –7.39 | — | 0.45 |
| **3b** | 3 | –6.82 | — | 1.34 |
| **3c** | 1 (top) | –6.89 | 8.92 | 0.00 |
| **3c** | 2 | –6.45 | — | 0.92 |
| **3c** | 3 | –6.21 | — | 1.45 |

[a] *Theoretical $K_i$ values calculated from ΔG at 298.15 K; intended for relative comparison only (typical AutoDock scoring uncertainty ≈ 1–2 kcal/mol).*

The lowest-energy poses nevertheless show different non-covalent interaction patterns (**Table 2** and **Figure 1a–c**).

**Table 2.** Non-covalent interactions between the top-ranked poses of **3a–c** and porcine aldose reductase (PDB ID: 1AH0), derived from 2D ligand-interaction analysis.

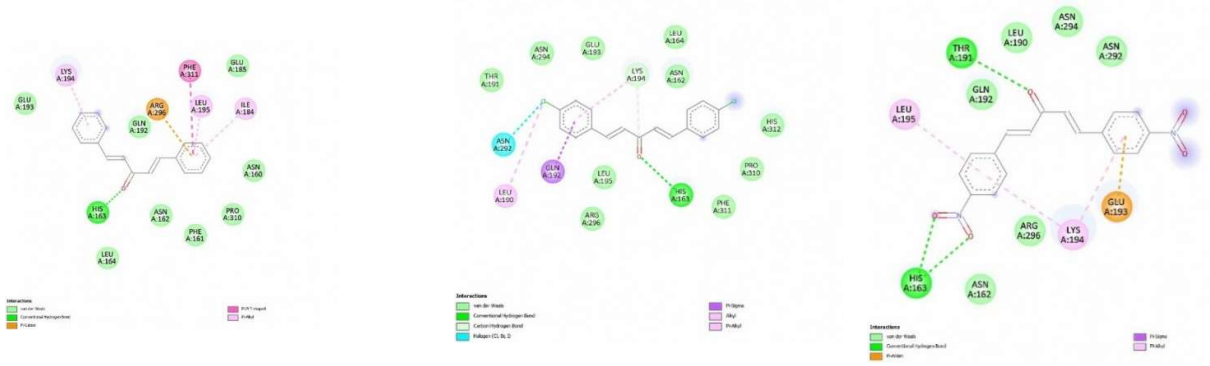
| Compound | Interaction Type | Interacting Residue(s) | Ligand Moiety |
|---|---|---|---|
| **3a** | Conventional H-bond | His163 | Carbonyl O |
| **3a** | π–Cation | Arg296 | Phenyl ring |
| **3a** | π–π T-shaped | Phe311 | Phenyl ring |
| **3a** | π–Alkyl | Leu195, Ile184 | Phenyl ring |
| **3a** | π–Alkyl | Lys194 | Phenyl ring |

| | | | |
|---|---|---|---|
| **3a** | van der Waals | Glu185, Glu193, Gln192, Asn160, Asn162, Leu164, Phe161, Pro310 | Binding pocket |
| **3b** | Conventional H-bond | His163 | Carbonyl O |
| **3b** | Carbon H-bond | Lys194 | Dienone C–H |
| **3b** | Halogen (Cl···O/N) | Asn292 | *p*-Cl substituent |
| **3b** | π–Sigma | Gln192 | 4-Chlorophenyl ring |
| **3b** | Alkyl / π–Alkyl | Leu190 (alkyl); Lys194 (π–alkyl) | *p*-Cl / 4-Chlorophenyl ring |
| **3b** | van der Waals | Thr190, Asn294, Glu193, Asn162, Leu164, Leu195, Arg296, His312, Pro310, Phe311 | Binding pocket |
| **3c** | Conventional H-bond | Thr190 | Carbonyl O |
| **3c** | Conventional H-bond | His163 | Nitro O atoms |
| **3c** | π–Anion | Glu193 | 4-Nitrophenyl ring |
| **3c** | π–Alkyl | Leu195, Lys194 | 4-Nitrophenyl rings |
| **3c** | van der Waals | Leu190, Asn294, Asn292, Gln192, Asn162, Arg296 | Binding pocket |

Unsubstituted DBA (**3a**) adopts an extended conformation in the binding pocket (**Figure 1a**). Its central carbonyl oxygen forms a conventional hydrogen bond with the imidazole side chain of His163, which is the main anchoring contact. One terminal phenyl ring forms a T-shaped π–π interaction with Phe311 and a π–cation contact with Arg296, and makes π–alkyl contacts with Leu195 and Ile184; the other phenyl ring makes a π–alkyl contact with Lys194. Further van der Waals contacts with Glu185, Glu193, Gln192, Asn160, Asn162, Leu164, Phe161 and Pro310 are also present.

In the 4,4′-dichloro analogue **3b**, the carbonyl oxygen again hydrogen-bonds to His163, and a weak carbon–hydrogen bond is formed between a dienone methine C–H and Lys194 (**Figure 1b**). One *para*-chlorine atom makes a contact with Asn292 that Discovery Studio classifies as a halogen interaction, and an alkyl contact with Leu190. A 4-chlorophenyl ring engages Gln192 in a π–σ interaction and Lys194 in a π–alkyl contact. The surrounding residues Thr191, Asn294, Glu193, Asn162, Leu164, Leu195, Arg296, His312, Pro310 and Phe311 form a dense network of van der Waals contacts.

The 4,4′-dinitro derivative **3c** adopts a somewhat more polar orientation (**Figure 1c**). The central carbonyl oxygen accepts a conventional hydrogen bond from Thr191, and the oxygen atoms of one *para*-nitro group form bifurcated hydrogen bonds with His163. The other 4-nitrophenyl ring, which is electron-poor because of the nitro group, interacts with the carboxylate side chain of Glu193 through a π–anion contact. Both rings also make π–alkyl contacts with Leu195 and Lys194, and the ligand is surrounded by van der Waals contacts with Leu190, Asn294, Asn292, Gln192, Asn162 and Arg296.



(**a**) 3a (**b**) 3b (**c**) 3c

***Figure 1.*** Two-dimensional ligand–protein interaction diagrams of the top-ranked docked poses of compounds 3a–c in the active site of porcine aldose reductase (PDB ID: 1AH0): (**a**) 3a — unsubstituted dibenzylideneacetone (HIS A:163 H-bond; ARG A:296 Pi–Cation; PHE A:311 Pi–Pi T-shaped; LYS A:194, LEU A:195, ILE A:184 Pi–Alkyl); (**b**) 3b — p,p′-dichloro dibenzylideneacetone (HIS A:163 H-bond; ASN A:292 halogen contact; GLN A:192 Pi–Sigma; LYS A:194, LEU A:190 Pi–Alkyl); (**c**) 3c — p,p′-dinitro dibenzylideneacetone (THR A:191 and HIS A:163 H-bonds; GLU A:193 Pi–Anion; LYS A:194, LEU A:195 Pi–Alkyl). Residue numbering follows the Discovery Studio Visualizer 2D diagrams of the prepared 1AH0 model.

These poses suggest that the central bis-enone unit fits well into the binding cavity of aldose reductase and that *para* substitution shifts the balance between halogen/hydrophobic anchoring (**3b**) and polar/electrostatic recognition (**3c**). These static poses are only a structural hypothesis. Whether the complexes are stable, and how strongly the compounds inhibit the enzyme, will have to be tested by molecular dynamics simulations in explicit solvent and by *in vitro* enzyme assays.

## 4. Conclusions

Dibenzylideneacetone (**3a**) and its 4,4′-dichloro (**3b**) and 4,4′-dinitro (**3c**) analogues were prepared by base-catalysed Claisen–Schmidt condensation in isolated yields of 52–65% and characterized by FT-IR, $^{1}$H and $^{13}$C NMR and UV–Vis spectroscopy; the data are consistent with the (1*E*,4*E*) configuration. Docking against porcine aldose reductase (PDB ID: 1AH0) gave predicted binding free energies of –6.89 to –7.43 kcal/mol and substituent-dependent interaction patterns in the binding pocket. The three compounds are readily accessible starting materials for the planned Schiff base derivatization at the

central carbonyl group, and the docking results provide a basis for testing them as aldose reductase inhibitors.

## References


[1] C. Zhuang, W. Zhang, C. Sheng, W. Zhang, C. Xing, Z. Miao, Chalcone: a privileged structure in medicinal chemistry, *Chem. Rev.* 117 (2017) 7762–7810. https://doi.org/10.1021/acs.chemrev.7b00020

[2] N.K. Sahu, S.S. Balbhadra, J. Choudhary, D.V. Kohli, Exploring pharmacological significance of chalcone scaffold: a review, *Curr. Med. Chem.* 19 (2012) 209–225. https://doi.org/10.2174/092986712803414132

[3] Raphaela P Guaringue, Vinicius M Schaffka, Larissa Kozan, André L Kerek, Eduardo Protachevicz, André V Bassani, Christiana A Pessoa, Patrícia M Campos, Guilherme A Camargo, Barbara C Fiorin,,. Chalcone Derivatives: Antioxidant Activity, Photoprotective Properties, and Stability under UV Irradiation. ACS Omega. 2025 Dec 15; 10 (51): 63061–63071. doi: 10.1021/acsomega.5c08934

[4] B.B. Popatkar, S. Yadav, S.B. Manjare, V.V. Borge, Green methods for the synthesis of chalcones: an overview with appraisal to sustainable development and bioactive compounds, *Org. Commun.* 18 (2025) 38–59. https://doi.org/10.25135/acg.oc.189.2504.3495

[5] A. Sousa, M. Lucas, D. Ribeiro, C.M. Correia, V.L.M. Silva, A.M.S. Silva, E. Fernandes, M. Freitas, Chalcones as modulators of neutrophil oxidative burst under physiological and high glucose conditions, *J. Nat. Prod.* 83 (2020) 3131–3140. https://doi.org/10.1021/acs.jnatprod.0c00728

[6] M. Faisal, Sonochemical protocol for solvent-free organic synthesis, in: *Green Sustainable Process for Chemical and Environmental Engineering and Science*, Elsevier, 2020, pp. 113–139. https://doi.org/10.1016/B978-0-12-819540-6.00005-X

[7] S. Prakash, G. Somiya, N. Elavarasan, K. Subashini, S. Kanaga, R. Dhandapani, M. Senthil Kumar, V. Sujatha, Synthesis and characterization of novel bioactive azo compounds fused with benzothiazole and their versatile biological applications, *J. Mol. Struct.* 1224 (2021) 129016. https://doi.org/10.1016/j.molstruc.2020.129016

[8] A. Urzhumtsev, F. Tête-Favier, A. Mitschler, J. Barbanton, P. Barth, L. Urzhumtseva, J.-F. Biellmann, A. Podjarny, D. Moras, A 'specificity' pocket inferred from the crystal structures of the complexes of aldose reductase with the pharmaceutically important inhibitors tolrestat and sorbinil, *Structure* 5 (1997) 601–612. https://doi.org/10.1016/S0969-2126(97)00216-5

[9] R. Maccari, R. Ottanà, Targeting aldose reductase for the treatment of diabetes complications and inflammatory diseases: new insights and future directions, *J. Med. Chem.* 58 (2015) 2047–2067. https://doi.org/10.1021/jm500907a



**აბსტრაქტი:**

დიბენზილიდენაცეტონი (DBA) და მისი ანალოგები ჯვარედინად შეუღლებულ ბის-ქალკონებს წარმოადგენენ. მათ ბიოლოგიური და ფოტოფიზიკური თვისებების ფართო სპექტრი ახასიათებთ. წინამდებარე ნაშრომში დიბენზალაცეტონი (3a) და მისი 4,4′-დიქლორ- (3b) და 4,4′-დინიტრო- (3c) ანალოგები მიღებულ იქნა აცეტონის (1) კონდენსაციით შესაბამის

პარა-ჩანაცვლებულ ბენზალდეჰიდებთან (**2a–c**) კლაიზენ–შმიდტის რეაქციის საფუძველზე. მიღებული პროდუქტები ეთილაცეტატიდან გადაკრისტალების შემდეგ გამოყოფილ იქნა 65% (**3a**), 57% (3b) და 52% (**3c**) გამოსავლიანობით. ინფრაწითელი სპექტროსკოპიისა და $^1$H პმრ მონაცემების საფუძველზე დადგენილ იქნა, რომ სამივე პროდუქტს აქვს (1E,4E)-კონფიგურაციას. ქლოროფორმში (10 მკგ/მლ) UV–Vis შთანთქმის მაქსიმუმები (λmax) დაფიქსირდა 330.6 ნმ-ზე (3a), 338 ნმ-ზე (3b) და 335 ნმ-ზე (**3c**). მოლეკულური დოკინგის მეთოდით შესწავლილ იქნა სინთეზირებული ნაერთების ურთიერთქმედება ღორის ალდოზა-რედუქტაზასთან (PDB ID: 1AH0) (პროგრამა AutoDock 4.2.6). პროგრამამ ჩვენა, რომ **3 a–c** ნაერთისთვის შეკავშირების თავისუფალი ენერგიები შესაბამისად –7.42, –7.43 და –6.89 კკალ/მოლ (სავარაუდო Ki 3.62, 3.58 და 8.92 მკმ). დადგინდა, რომ ნაერთი **3a** His163-თან წყალბადურ ბმას წარმოქმნის, ხოლო მისი არომატული სისტემა Phe 311-თან π–π T-ფორმის, ARG296-თან π–კატიონურ და Leu195-, Ile 184- და Lys 194-თან π–ალკილურ ურთიერთქმედებებს ახორციელებს**. 3b** წყალბადურ ბმას წარმოქმნის His163-თან, Cl···O/N ჰალოგენურ კავშირს Asn 292-თან, აგრეთვე π–σ და π–ალკილურ ურთიერთქმედებებს; ხოლო **3c** წყალბადურ ბმებს წარმოქმნის Thr191-სა და His163-თან და π–ანიონურ კონტაქტს Glu193-თან. რადგან შეკავშირების თავისუფალი ენერგიის მნიშვნელობებს შორის განსხვავება 0.01–0.54 კკალ/მოლია, რაც დოკინგის პროგრამის მიახლოებითი გამოთვლებისთვის დამახასიათებელ ცდომილებაზე (დაახლოებით 1–2 კკალ/მოლ) ნაკლებია, სამივე ნაერთი სავარაუდო აფინობის თვალსაზრისით თანაბრად უნდა ჩაითვალოს. დოკინგის მოდელები მოლეკულური დინამიკის სიმულაციებისა და ალდოზა-რედუქტაზას ინჰიბირების *in vitro* კვლევებისთვის საწყის წერტილს წარმოადგენს.

***საკვანძო სიტყვები:*** დიბენზალაცეტონი, კლაიზენ-შმიდტის რეაქცია, ბის-ქალკონები, მოლეკულური დოკინგი, ალდოზა რედუქტაზა